Shortcuts in domain walls and the horizon problem

Elcio Abdalla and Bertha Cuadros-Melgar
Instituto de Fisica, Universidade de São Paulo, C.P. 66.318, CEP 05315-970, São Paulo, Brazil
(Received 12 September 2002; published 21 April 2003)

We consider a dynamical membrane world in a space-time with scalar bulk matter described by domain walls. Using the solutions to Einstein field equations and Israel conditions we investigate the possibility of having shortcuts for gravitons leaving the wall and returning subsequently. As it turns out, they usually appear under mild conditions. In the comparison with photons following a geodesic inside the brane, we verify that shortcuts exist. For some universes they are small, but there are cases where shortcuts are effective. In these cases we expect them to play a significant role in the solution of the horizon problem.

DOI: 10.1103/PhysRevD.67.084012 PACS number(s): 04.50.+h, 98.80.Jk, 11.27.+d, 11.10.Kk

I. INTRODUCTION

Although the standard model of particle physics has been established as the uncontested theory of all interactions down to distances of 10^{-17} m, there are good reasons to believe that there is a new physics arising soon at the experimental level [1]. On the other hand, string theory provides an excellent background to solve long-standing problems of theoretical high-energy physics. It is by now a widespread idea that M-theory [2] is a reasonable description of our Universe. In the field theory limit, it is described by a solution of the (eventually 11-dimensional) Einstein equations with a cosmological constant by means of a four-dimensional membrane. In this picture only gravity survives in the extra dimensions, while the remaining matter and gauge interactions are typically four dimensional.

In this picture, there is a possibility that gravitational fields, while propagating out of the brane speed up, reaching farther distances in smaller time as compared to light propagating inside the brane, a scenario that for a resident of the brane (as ourselves) implies shortcuts [3–8].

This possibility implies that we can have alternatives to the inflationary scenario in order to explain the homogeneity problem in cosmology. Recently, this scenario has been proposed as an actually realizable possibility [9–12]. In Ref. [11] it has been shown that in some scenarios shortcuts are very difficult to detect today because of the extremely short delay of the photon as compared to the graviton coming from the same source. However, in cases where before nucleosynthesis delays are large enough to imply thermalization of the whole universe, a possible solution to the homogeneity problem [11], alternative [9,10,12] to inflation [13], may exist based on these shortcuts. In the case of domain walls shortcuts are common and the possibility of solving the homogeneity problem may be under way, though further work is certainly necessary.

Recently it has been proved [14] that brane Universes can provide a means for finding relics of the higher dimensions in the cosmic microwave background as well [23]. Thus it is worthwhile further pursuing brane models as useful tools to understand the physics of strings and M-theory [15], which proves them as very important instances to discover a better insight of the Universe and its properties.

At last, we should stress that this is a toy model where the universe is replaced by a domain wall. The more realistic case deserves attention as well (see also Refs. [11,19–22]).

II. GENERAL SETUP

We consider a scenario described by the gravitational action in a D-dimensional bulk with a scalar field, a bulk dilaton, a domain-wall potential, and a Gibbons-Hawking term [16],

$$S=\int_{bulk} d^Dx\sqrt{-g}\left(\frac{1}{2}R-\frac{1}{2}(\partial\phi)^2-V(\phi)\right)$$
$$-\int_{dw} d^{D-1}x\sqrt{-h}\{[K]+\hat{V}(\phi)\}, \tag{1}$$

where ϕ is the bulk dilaton, K is the extrinsic curvature, $V(\phi)$ and $\hat{V}(\phi)$ are bulk and domain-wall potentials, respectively, and g and h denote the bulk and domain-wall metrics. The potentials are here considered to be of the Liouville type:

$$V(\phi)=V_0e^{\beta\phi}, \tag{2}$$

$$\hat{V}(\phi)=\hat{V}_0e^{\alpha\phi}. \tag{3}$$

We consider the bulk metric as being static and invariant under rotation, being given by

$$ds^2=-U(r)dt^2+U(r)^{-1}dr^2+R(r)^2\,d\Omega_k^2, \tag{4}$$

where $d\Omega_k^2$ is the line element on a $D-2$-dimensional space of constant curvature depending on a parameter k. Such a metric is supposed to have a mirror symmetry Z_2 with respect to the domain wall. Such a symmetry will be used in order to impose the Israel conditions [17]. In fact, the variation of the total action (1) including the Gibbons-Hawking term leads directly to the Israel conditions which in view of the Z_2 symmetry become

$$K_{MN}=-\frac{1}{2(D-2)}\hat{V}(\phi)h_{MN}. \tag{5}$$

The extrinsic curvature can be computed as

$$K_{MN}=h_M^P h_N^Q \nabla_P n_Q, \tag{6}$$

where the unit normal, which points into $r<r(t)$, is

$$n_M=\frac{1}{\sqrt{U-\frac{\dot{r}^2}{U}}}(\dot{r},-1,0,\ldots,0). \tag{7}$$

Here a dot means derivative with respect to the bulk time t.

The ij component of Eq. (5) can be written as

$$\frac{R'}{R}=\frac{\hat{V}(\phi)}{2(D-2)U}\sqrt{U-\frac{\dot{r}^2}{U}}, \tag{8}$$

while the 00 component is

$$\left(\frac{R'}{R}\right)^{-1}\left(\frac{R'}{R}\right)'=\frac{\hat{V}'(\phi)}{\hat{V}(\phi)}-\frac{R'}{R}. \tag{9}$$

Here a prime denotes derivative with respect to the radial extra coordinate r.

The equation of motion for the dilaton obtained from the action (1), together with Eq. (9), can be simultaneously solved with the ansatz (4), leading to [18]

$$\phi(r)=\phi_\star-\frac{\alpha(D-2)}{\alpha^2(D-2)+1}\log r, \tag{10}$$

$$R(r)=[\alpha^2(D-2)+1]C\hat{V}_0 e^{\alpha\phi_\star} r^{1/[\alpha^2(D-2)+1]}, \tag{11}$$

where $\phi_\star$ and C are arbitrary integration constants.

The motion of the domain wall is governed by the ij component of the Israel conditions (8). That equation can be written in terms of the brane proper time τ as

$$\frac{1}{2}\left(\frac{dR}{d\tau}\right)^2+F(R)=0. \tag{12}$$

The induced metric on the domain wall is Friedmann-Robertson-Walker and Eq. (12) describes the evolution of the scale factor $R(\tau)$. This equation is the same as the one for a particle of unit mass and zero energy rolling in a potential $F(R)$ given by

$$F(R)=\frac{1}{2}UR'^2-\frac{1}{8(D-2)^2}\hat{V}^2R^2. \tag{13}$$

Notice that the solution only exists when $F(R)\leqslant 0$.

From the induced domain-wall metric we find the relations between the time parameter on the brane (τ) and in the bulk (t) as given by

$$dt=\frac{\sqrt{U+\left(\frac{dr}{d\tau}\right)^2}}{U}d\tau,$$

so that

$$\dot{r}\equiv\frac{dr}{dt}=\frac{dr}{d\tau}\frac{d\tau}{dt}=\frac{dr}{d\tau}\frac{U}{\sqrt{U+\left(\frac{dr}{d\tau}\right)^2}}, \tag{14}$$

where $dr/d\tau=(dR/d\tau)(dR/dr)^{-1}$ can be obtained from Eq. (12). Equation (14) describes the motion of a domain wall in the static background as seen by an observer in the bulk.

Consider two points on the brane. In general, there is more than one null geodesic connecting them in the D-dimensional spacetime. The trajectories of photons must be on the brane and those of gravitons may be outside. We consider the shortest path for both photons and gravitons. For the latter, the geodesic equation is the same as the one considered in Ref. [3], since the bulk metric is static:

$$\ddot{r}_g+\left(\frac{1}{r_g}-\frac{3}{2}\frac{U'}{U}\right)\dot{r}_g^2+\frac{1}{2}UU'-\frac{U^2}{r_g}=0. \tag{15}$$

Again a dot means a derivative with respect to the bulk time t.

The solutions of Eqs. (14) and (15) in terms of the bulk proper time t were obtained by means of a MAPLE program. Now we discuss the possibility of shortcuts in the cases of the various solutions describing different Universes defined by the domain-wall solution.

III. SOLUTIONS OF THE GEODESIC EQUATION

A. Type-I solutions

We define the type-I brane solutions as those for which $\alpha=\beta=0$. Consequently, the potentials become cosmological constants. The solution also has a constant dilaton $\phi=\phi_0$. A simple rescaling in the metric leads us to

$$ds^2=-U(R)dt^2+U(R)^{-1}dR^2+R^2\,d\Omega_k^2, \tag{16}$$

with

$$U(R)=k-2MR^{-(D-3)}-\frac{2V_0}{(D-1)(D-2)}R^2, \tag{17}$$

which corresponds to a topological black hole solution in D dimensions with a cosmological constant.

As discussed in Ref. [18], if the domain wall has positive energy density ($\hat{V}_0>0$), the relevant part of the bulk spacetime is $R<R(\tau)$, which is the region containing the singularity. If it has negative energy density ($\hat{V}_0<0$), the relevant part is $R>R(\tau)$, which is nonsingular unless the wall reaches $R=0$.

The potential $F(R)$ ruling the evolution of the scale factor is

$$F(R)=\frac{k}{2}-MR^{-(D-3)}-\hat{\Lambda}R^2, \tag{18}$$

where the effective cosmological constant on the domain wall is given by

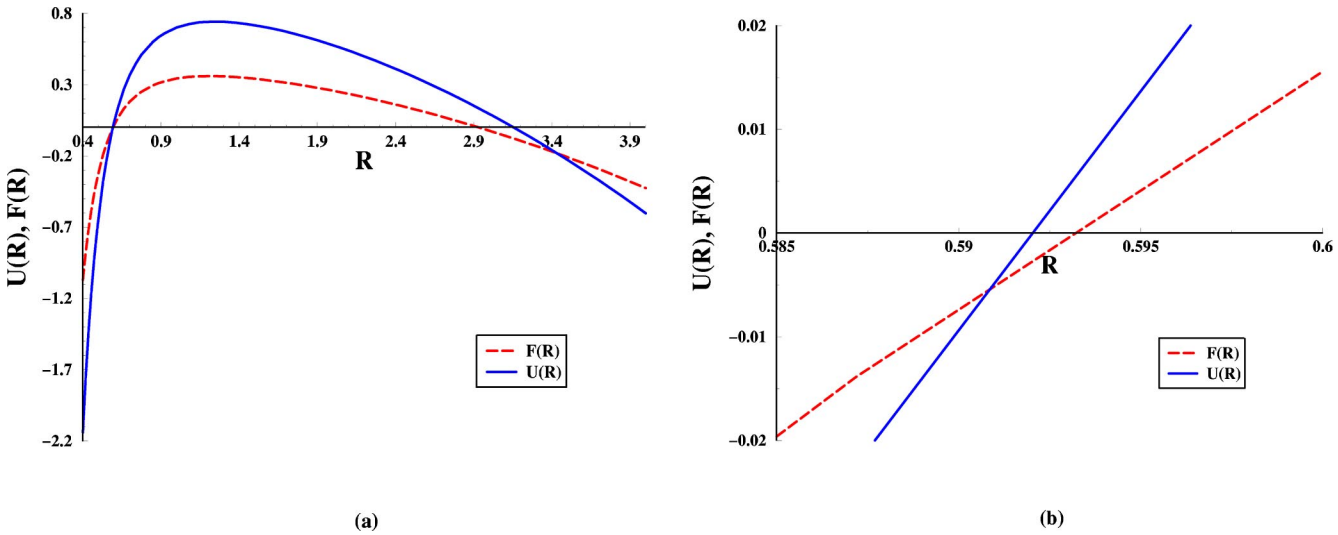

FIG. 1. (a) $U(R)$ and $F(R)$ for type-I solutions with $M=1/10$, $V_0=1$, and $\hat{V}_0=\pm 1$. (b) Zoom of the event horizon region.

$$\hat{\Lambda}=\frac{1}{D-2}\left[\frac{V_0}{D-1}+\frac{\hat{V}_0^2}{8(D-2)}\right]. \tag{19}$$

We shall analyze each of the four cases presented in Ref. [18]. As we have previously stated, the equation of motion (12) has a solution only when $F(R)\leqslant 0$. This is automatic only if $U(R)<0$, i.e., if r is a time coordinate; therefore we look for solutions with $U(R)>0$. In fact, both conditions,

$$F(R)\leqslant 0 \quad \text{and} \quad U(R)>0, \tag{20}$$

can coexist in some cases as we will see in what follows. In order to illustrate the following examples we have chosen $D=6$ dimensions.

1. $\hat{\Lambda}>0$, $M>0$

From the graph of $U(R)$ (see Fig. 1) we can choose the initial condition for the domain wall assuming that Eq. (17) describes a de Sitter– (dS-)Schwarzschild bulk with event and cosmological horizons when $M>0$ and $V_0>0$.

We thus choose the initial condition for the domain wall inside this region and where r is a space coordinate. From Fig. 1 let us notice that there are two small regions, $r_H\leqslant r<0.593$ and $2.93\leqslant r<r_C$, where Eq. (20) holds. The results are shown in Fig. 2. We see that for region I the geodesics follow the domain wall for a while and then decouple falling into the event horizon. For region II all the geodesics and the domain wall converge to the cosmological horizon r_C independently of the value of $\hat{V}_0$.

2. $\hat{\Lambda}<0$, $M>0$

This case describes an anti-de Sitter– (AdS-)Schwarzschild bulk. The condition (20) is fulfilled inside a very small range as we can see in Fig. 3(a). However, all the geodesics fall into the event horizon after following some path on the brane [see Fig. 3(b)].

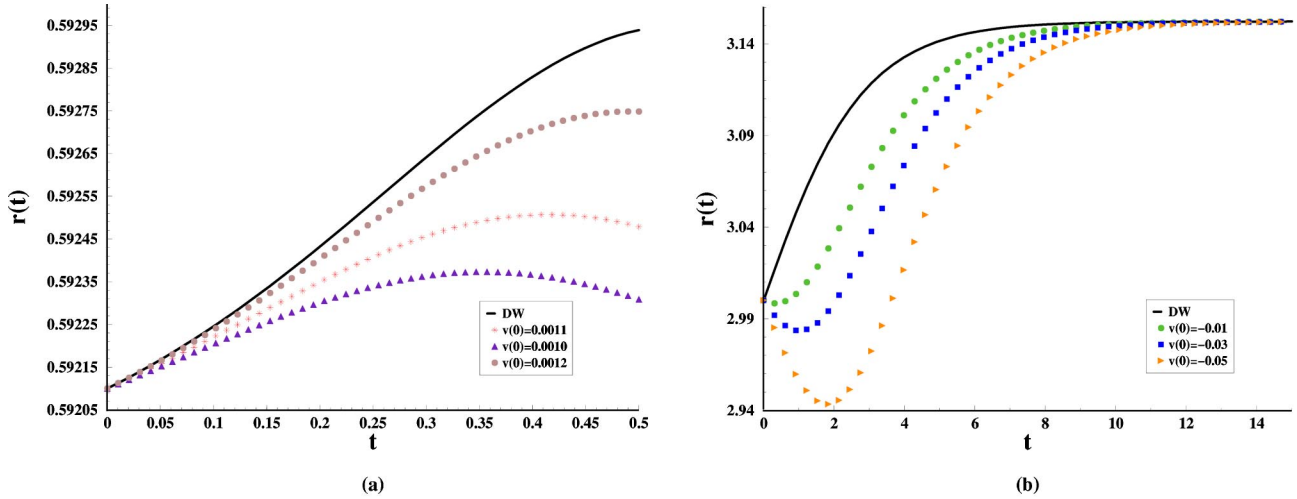

FIG. 2. Domain-wall motion and geodesics for type-I solutions with $M=1/10$, $V_0=1$, and $\hat{V}_0=1$ in (a) region I and (b) region II.

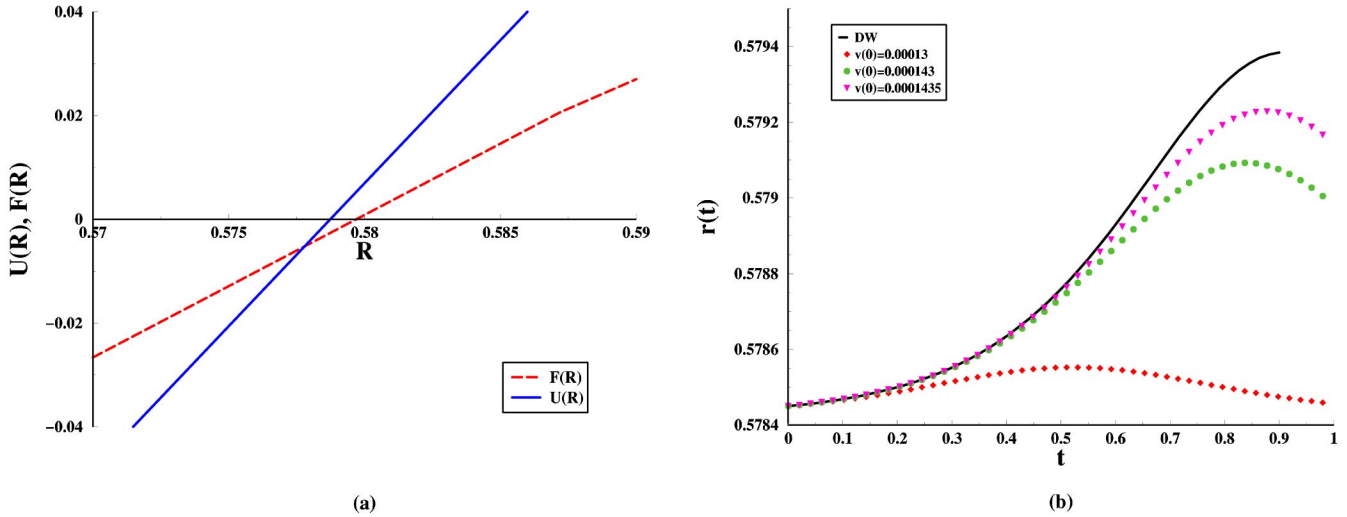

(a) (b)

FIG. 3. (a) Zoom of the region where Eq. (20) holds from the graph of $U(R)$ and $F(R)$ with $\hat{\Lambda}<0$ and $M>0$ for type-I solutions. (b) Domain-wall motion and geodesics for type-I solutions with $M=1/10$, $V_0=-1$, and $\hat{V}_0=1$.

3. $\hat{\Lambda}>0$, $M<0$

From Fig. 4(a) we choose the initial condition for the domain-wall equation of motion inside the region where Eq. (20) holds. As we can see from Fig. 4(b), the domain wall and the geodesic converge to the cosmological horizon r_C. However, after some threshold initial velocity the geodesics diverge to the timelike naked singularity.

4. $\hat{\Lambda}<0$, $M<0$

In this case Eq. (12) can only have a solution when $k=-1$. This is a topological black hole in an asymptotically AdS space. From Fig. 5 we see that there is no solution satisfying Eq. (20) between event and cosmological horizons.

B. Type-II solutions

The type-II solutions have $\alpha=\beta/2$ and $k=0$. The metric is given by

$$U(r)=(1+b^2)^2 r^{2/(1+b^2)} \times\left(-2Mr^{-(D-1-b^2)/(1+b^2)}-\frac{2\Lambda}{(D-1-b^2)}\right), \tag{21}$$

and the scale factor is

$$R(r)=r^{1/(1+b^2)}, \tag{22}$$

where

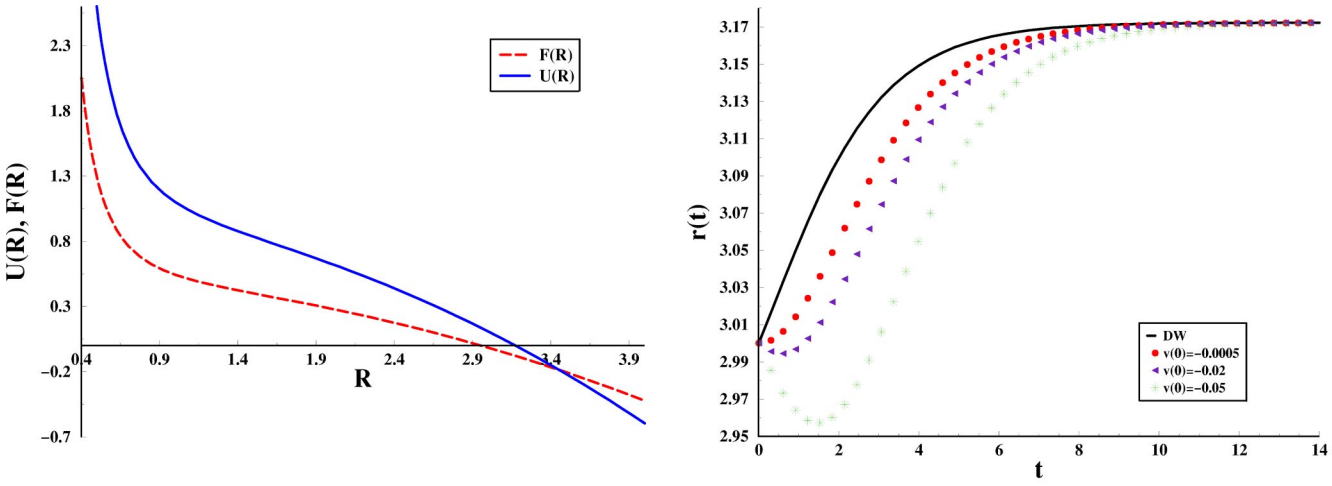

(a) (b)

FIG. 4. (a) $U(R)$ and $F(R)$ with $\hat{\Lambda}>0$ and $M<0$ for type-I solutions. (b) Domain-wall motion and geodesics for $M=-1/10$, $V_0=1$, and $\hat{V}_0=1$.

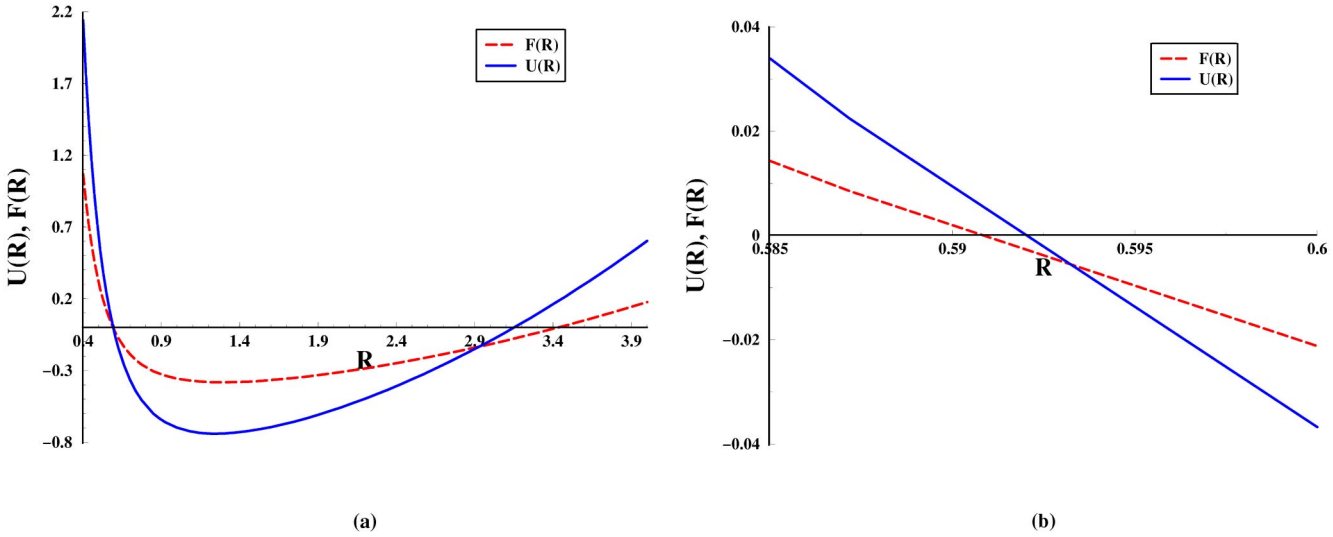

FIG. 5. (a) $U(R)$ and $F(R)$ with $\hat{\Lambda}<0$ and $M=-1/10$ for type-I solutions. (b) Zoom of the event horizon region.

$$\Lambda=\frac{V_0 e^{2b\phi_0}}{D-2}, \tag{23}$$

$$b=\frac{1}{2}\beta\sqrt{D-2}. \tag{24}$$

The potential is given by the expression

$$F(R)=-R^{2(1-b^2)}(MR^{-(D-1-b^2)}+\hat{\Lambda}), \tag{25}$$

where

$$\hat{\Lambda}=\frac{e^{2b\phi_0}}{D-2}\left(\frac{V_0}{D-1-b^2}+\frac{\hat{V}_0^2}{8(D-2)}\right). \tag{26}$$

There are 12 cases from which we choose those ones where r is a spatial coordinate. When $b^2<D-1$, r is a spatial coordinate if $V_0<0$. When $b^2>D-1$, r is spatial if $M<0$.

We should also rewrite Eq. (20) as

$$F(r)\leqslant 0 \quad \text{and} \quad U(r)>0. \tag{27}$$

1. $\hat{\Lambda}>0$, $M<0$, $b^2>D-1$

In this case $U(r)$ is always positive, whereas $F(r)$ is negative for small r. From Fig. 6 we see that some microscopic shortcuts appear in the very beginning of the solution and after crossing the domain wall they escape to infinity.

2. $\hat{\Lambda}<0$, $M>0$, $b^2<1$

This case describes a black $(D-2)$ brane solution in AdS space. Here there is a very small region where Eq. (27) holds

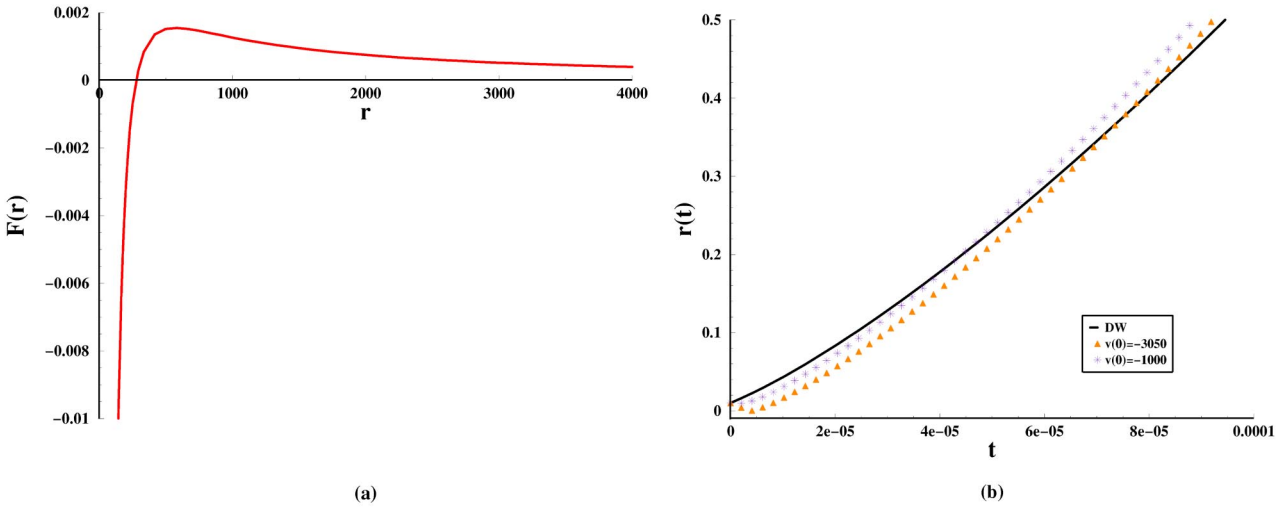

FIG. 6. (a) $F(r)$ with $\hat{\Lambda}>0$ and $M<0$ for type-II solutions. (b) Domain-wall motion and geodesics for $V_0=1$, $\hat{V}_0=6$, $M=-10$, and $\beta=\sqrt{10}$.

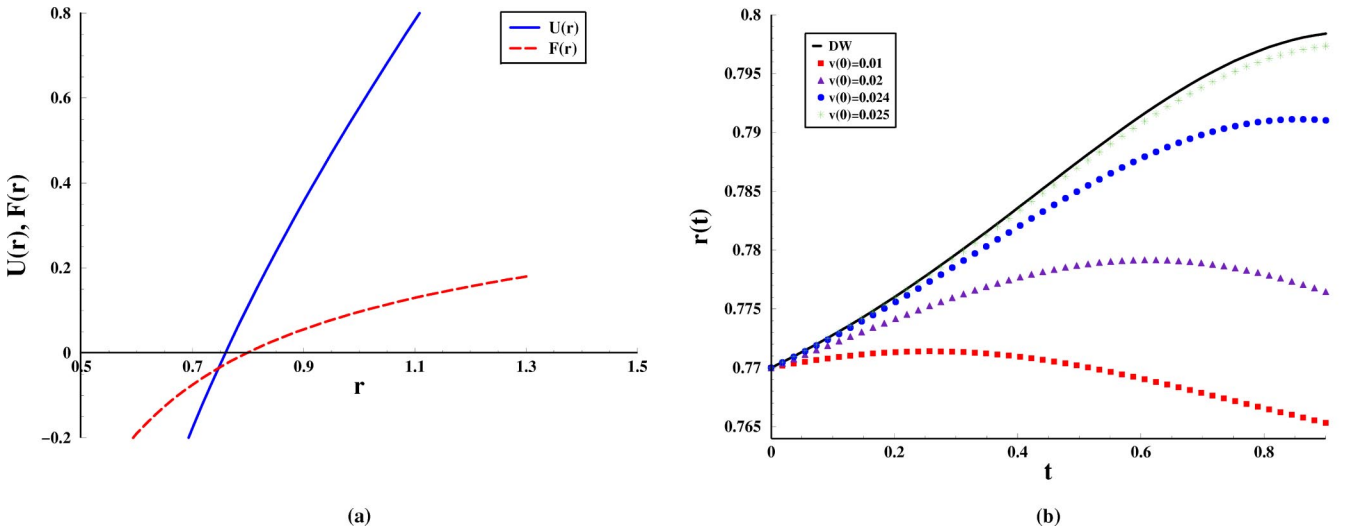

(a) (b)

FIG. 7. (a) $U(r)$ and $F(r)$ with $\hat{\Lambda}<0$ and $M>0$ for type-II solutions. (b) Domain-wall motion and geodesics for $V_0=-1$, $\hat{V}_0=1$, $M=1/10$, and $\beta=1/\sqrt{2}$.

after the event horizon as we can see from Fig. 7. We show the entire domain wall solution and we see that geodesics follow it and then decouple to fall into the event horizon at later times.

3. $\hat{\Lambda}<0$, $M>0$, $1<b^2<D-1$

This case is also a black brane in AdS space. The region where Eq. (27) is respected is shown in Fig. 8. As in the previous case all the geodesics follow the domain wall and at later times fall into the event horizon.

4. $\hat{\Lambda}<0$, $M<0$

As $F(r)$ is always positive for all b^2, no solutions to Eq. (14) exist.

C. Type-III solutions

The type-III solutions have $\alpha=2/\beta(D-2)$. In this case, the metric is given by

$$U(r)=(1+b^2)^2 r^{2/(1+b^2)} \times\left(-2Mr^{[-1+b^2(D-3)]/(1+b^2)}-\frac{2\Lambda}{[1+b^2(D-3)]}\right), \tag{28}$$

and the scale factor is

$$R(r)=\gamma r^{b^2/(1+b^2)}, \tag{29}$$

where

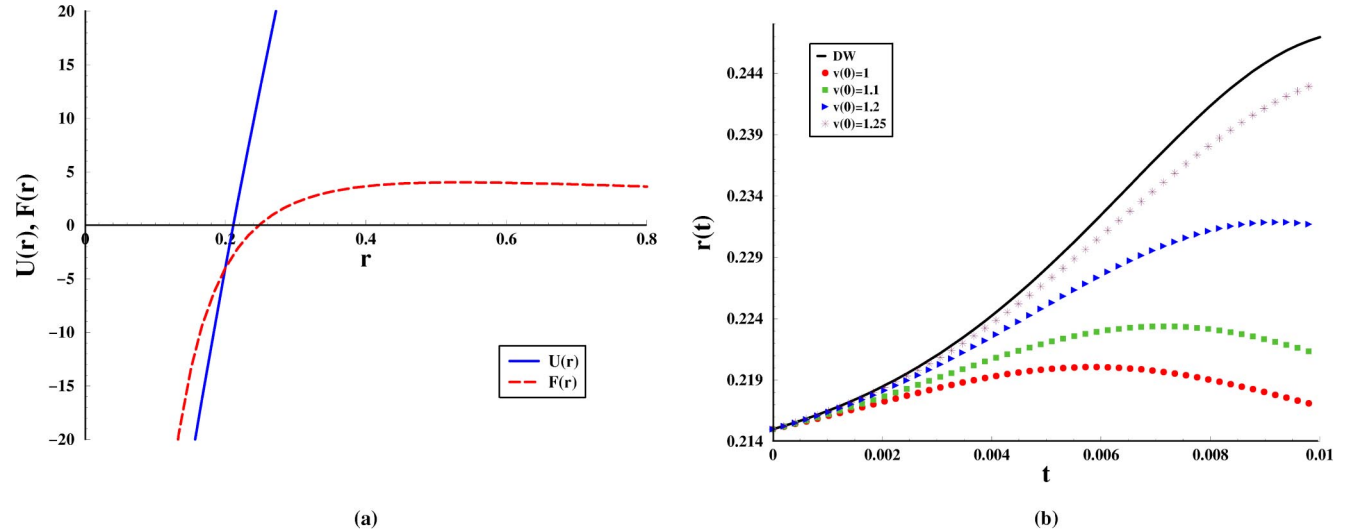

(a) (b)

FIG. 8. (a) $U(r)$ and $F(r)$ with $\hat{\Lambda}<0$ and $M>0$ for type-II solutions. (b) Domain-wall motion and geodesics for $V_0=-1$, $\hat{V}_0=1$, $M=10$, and $\beta=2$.

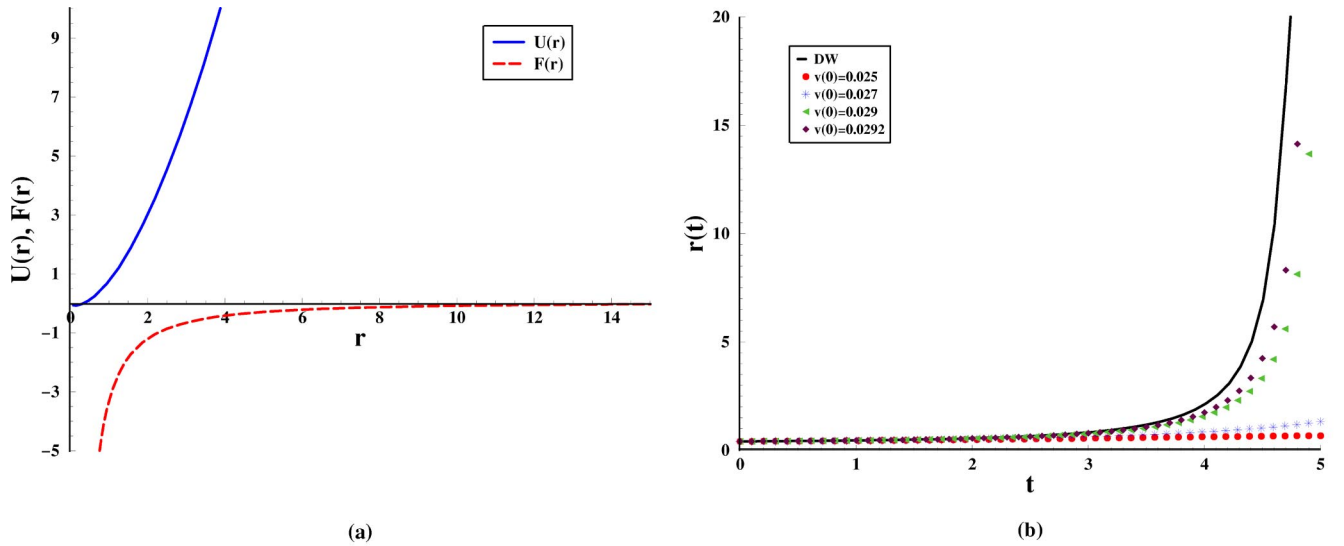

FIG. 9. (a) $U(r)$ and $F(r)$ for type-III solutions with $k=-1$, $M=1/10$, and $\beta^2<1/(D-2)$. (b) Domain-wall motion and geodesics for $V_0=-1$, $\hat{V}_0=1$, $\phi_0=1$, and $\beta=1/\sqrt{6}$.

$$\gamma=\left(\frac{(D-3)}{2k\Lambda(1-b^2)}\right)^{1/2}. \tag{30}$$

The values of Λ and b are the same as those given in Eqs. (23) and (24).

The potential $F(R)$ is

$$F(R)=-\frac{(D-3)b^4}{2k(1-b^2)[1+b^2(D-3)]} -M\gamma^2 b^4\left(\frac{R}{\gamma}\right)^{-(D-3+1/b^2)} -\frac{\hat{V}_0^2 e^{2\phi_0/b}\gamma^2}{8(D-2)^2}\left(\frac{R}{\gamma}\right)^{-2(1/b^2-1)}. \tag{31}$$

If $V_0>0$, r turns out to be a time coordinate, while for $V_0<0$, it is a spatial coordinate. From the 12 cases shown in Ref. [18] we choose those where it is a spatial coordinate. For all these solutions the condition (27) applies.

1. $V_0<0$, $M>0$, $b^2<1/(D-1)$

This case describes a topological black hole in AdS space. From Fig. 9 we can see the region where Eq. (27) holds. There are no shortcuts in this interval, and all the geodesics follow the brane and then either diverge to infinity or fall into the event horizon.

2. $V_0<0$, $M>0$, $1/(D-1)<b^2<1$

We again have a topological black hole in AdS space. There is a small interval where Eq. (14) has solution as we

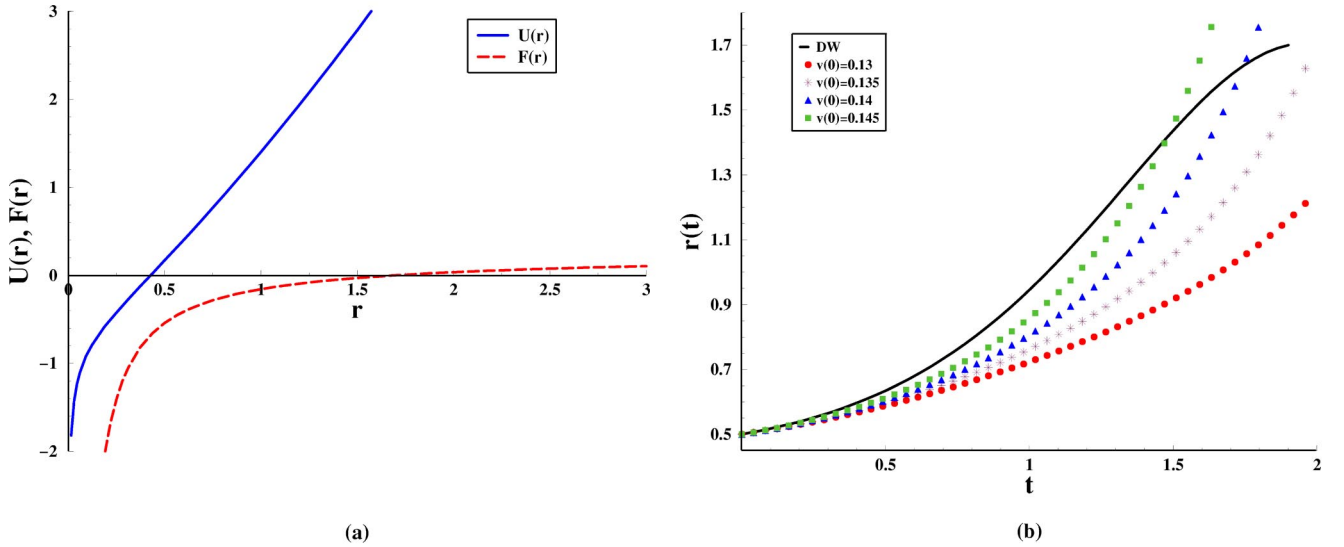

FIG. 10. (a) $U(r)$ and $F(r)$ for $k=-1$, $M=1/10$, and $V_0<0$ in type-III solutions. (b) Domain-wall motion and geodesics with $V_0=-1$, $\hat{V}_0=1$, $\phi_0=1$, and $\beta=1/\sqrt{2}$.

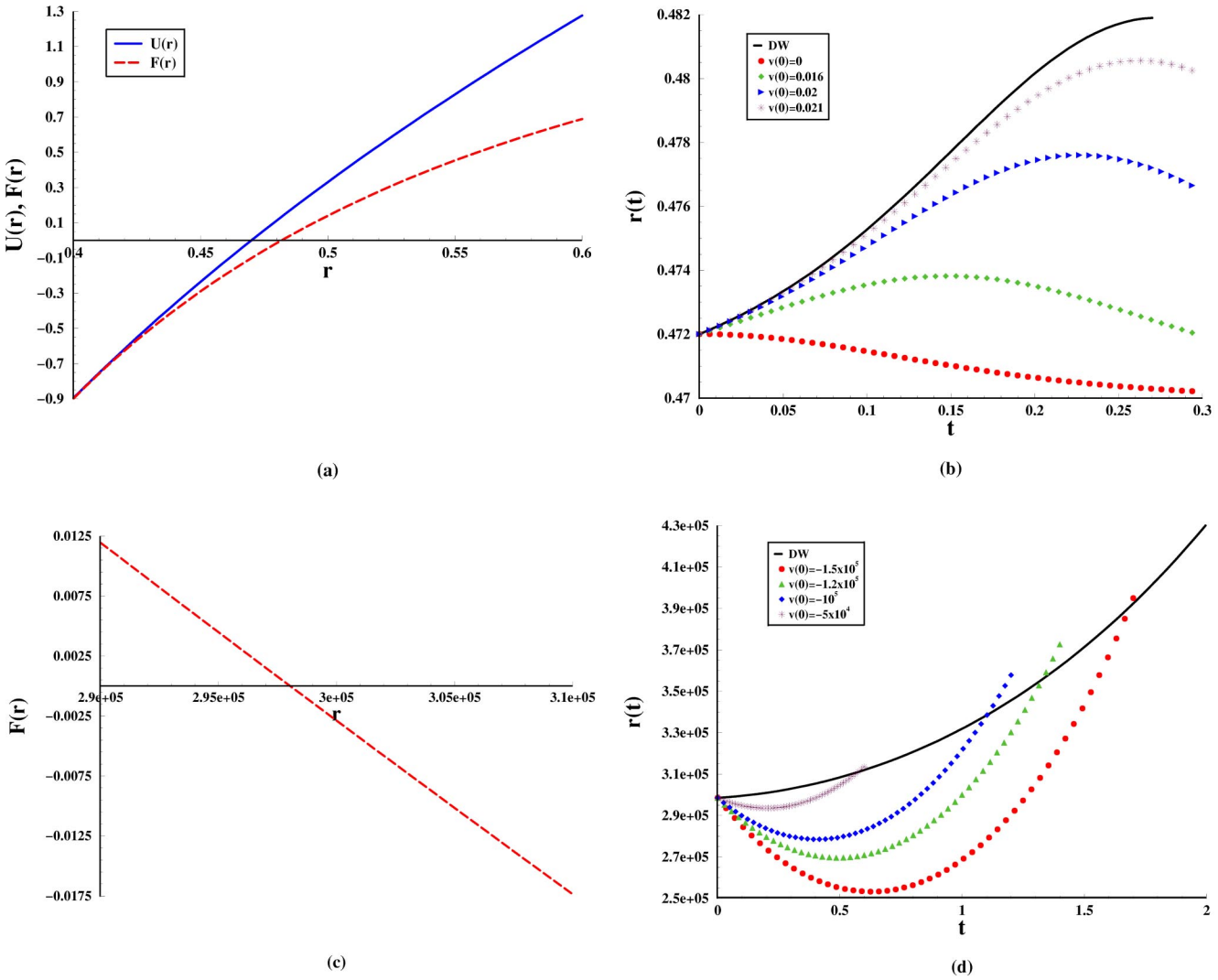

FIG. 11. (a) $U(r)$ and $F(r)$ for $M=1/10$ and $V_0<0$ in type-III solutions. (b) Domain-wall motion and geodesics with $V_0=-1$, $\hat{V}_0=1$, $\phi_0=1$, and $\beta=\sqrt{5}/2$. (c) $F(r)$ in the region of interest. (d) Domain-wall motion and geodesics under the same conditions as (b).

can see from Fig. 10(a). Our results are shown in Fig. 10(b). Notice that the domain-wall equation of motion has a solution only inside the interval shown there. This means that only a group of geodesics with initial velocity $\dot{r}(0)>v_c$ can meet the domain wall after a roundabout in the bulk. It is also shown that negative initial velocities force geodesics to fall into the event horizon.

3. $V_0<0$, $M>0$, $b^2>1$

The black hole in AdS space appearing here has a round spatial section. In this case $U(r)$ is always positive (then r is always a spatial coordinate); however, as we must fulfill Eq. (27), we should notice that $F(r)\leqslant 0$ for $r\geqslant 3\times 10^5$. We found that shortcuts are possible for several initial velocities if $M=0$.

The case $M>0$ is shown in Fig. 11. We have two regions of interest after the event horizon depending only on the sign of $F(r)$ since $U(r)$ is positive in this range. In the first region all the geodesics initially follow the brane and fall into the event horizon at later times. In the second region we have shortcuts again for several initial velocities.

4. $V_0<0$, $M<0$, $b^2<1/(D-1)$

Here $U(r)$ is always positive while $F(r)$ is negative in the range shown in Fig. 12. The domain wall and the geodesics diverge after some time near the end of the range where Eq. (14) has a solution.

5. $V_0<0$, $M<0$, $1/(D-1)<b^2<1$

In this case $U(r)$ is always positive while $F(r)$ is negative for a small range as seen in Fig. 13. There are several shortcuts in the region where the domain-wall equation of motion has solution; nevertheless, there is a threshold velocity after which the geodesics cannot return. As we can notice from Fig. 13(b), the last curve displayed here $[v(0)=-1.04]$ cannot be considered a real shortcut since it is not a continuous solution of the geodesic equation, but represents a transition between shortcuts and geodesics falling into the naked singularity.

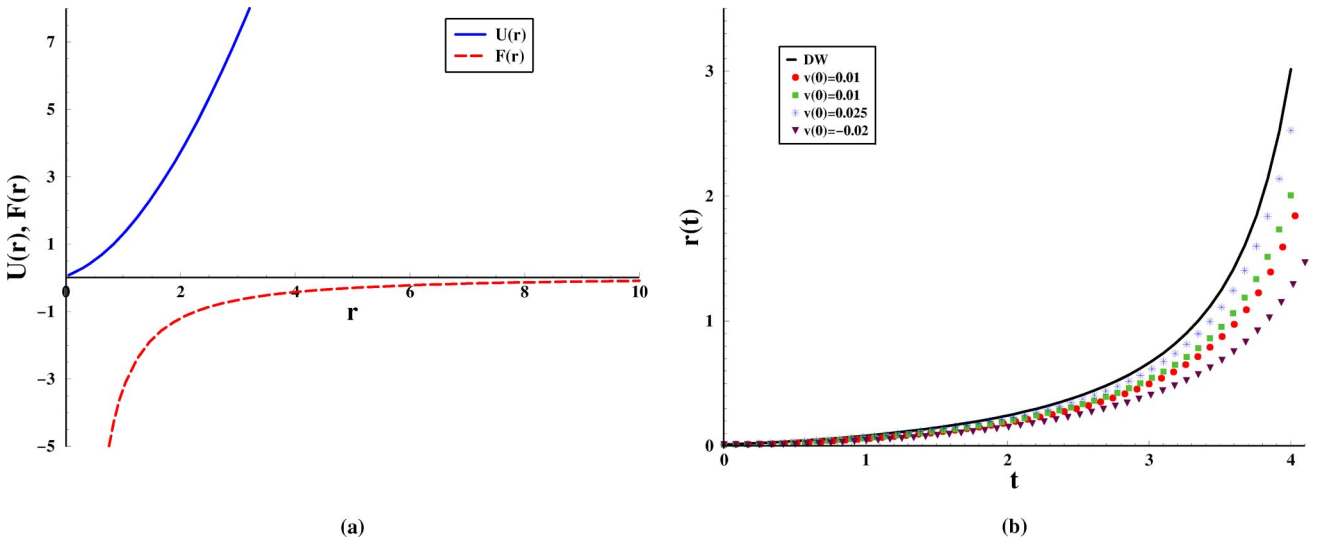

FIG. 12. (a) $U(r)$ and $F(r)$ for type-III solutions when $k=-1$, $M=-1/10$, and $b^2<1/(D-2)$. (b) Domain-wall motion and geodesics for $V_0=-1$, $\hat{V}_0=1$, $\phi_0=1$, and $\beta=1/\sqrt{6}$.

6. $V_0<0$, $M<0$, $b^2>1$

Now $U(r)$ is always positive and $F(r)$ will determine the initial condition for the domain-wall equation of motion. As we can see from Fig. 14, several shortcuts appear.

IV. DOMAIN-WALL TIME AND TIME DELAYS

The time delay between the photon traveling on the domain wall and the gravitons traveling in the bulk [11] can be calculated as follows. Since the signals cover the same distance,

$$\int \frac{d\tau_\gamma}{r(\tau_\gamma)} = \int \frac{dt_g}{r_g(t_g)} \sqrt{U(r_g) - \frac{\dot{r}_g(t)^2}{U(r_g)}}, \tag{32}$$

the difference between photon and graviton time of flight can approximately be written as

$$\frac{\Delta\tau}{r} \simeq \int_0^{\tau_f+\Delta\tau} \frac{d\tau_\gamma}{r(\tau_\gamma)} - \int_0^{\tau_f} \frac{d\tau_g}{r(\tau_g)}, \tag{33}$$

or in terms of the bulk time

$$\Delta\tau \simeq r(t_f) \int_0^{t_f} dt \left(\frac{1}{r_g(t)} \sqrt{U(r_g) - \frac{\dot{r}_g(t)^2}{U(r_g)}} - \frac{1}{r(t)} \frac{d\tau}{dt} \right). \tag{34}$$

The elapsed bulk time t, the corresponding domain-wall time τ, and the delays (34) are shown in Table I for all the shortcut examples considered in the present paper. Notice that $\Delta\tau<0$ for the last geodesic solution in Fig. 13 which, in fact,

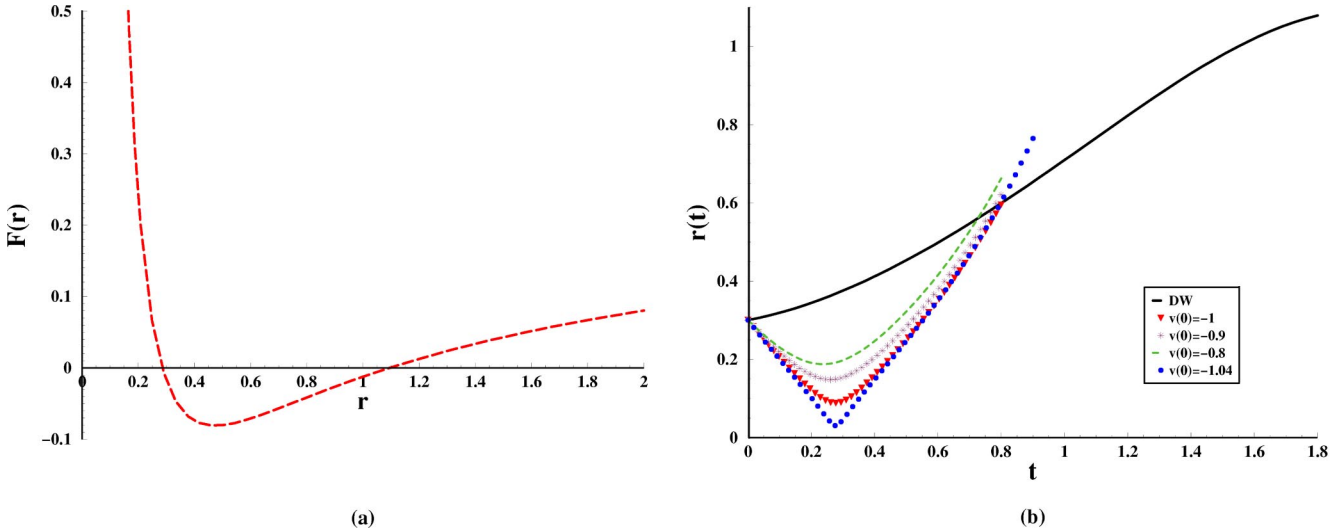

FIG. 13. (a) $F(r)$ for type-III solutions when $k=-1$, $M=-1/10$, and $1/(D-2)<b^2<1$. (b) Domain-wall motion and geodesics for $V_0=-1$, $\hat{V}_0=1$, $\phi_0=1$, and $\beta=1/\sqrt{2}$.

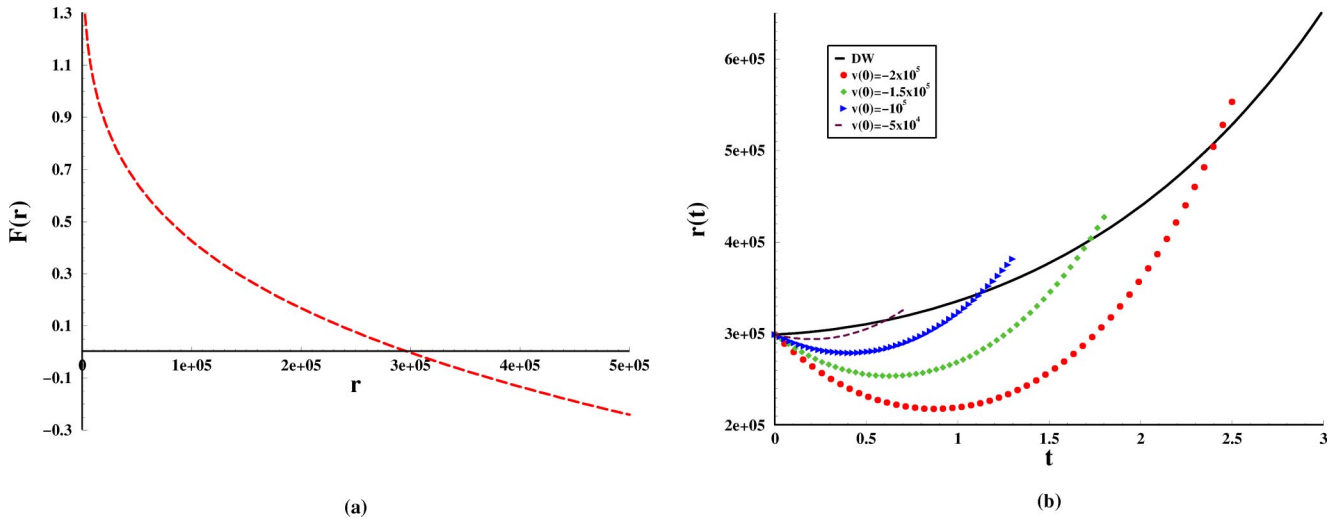

FIG. 14. (a) $F(r)$ for type-III solutions when $M=-1/10$ and $b^2>1$. (b) Domain-wall motion and geodesics for $V_0=-1$, $\hat{V}_0=1$, $\phi_0=1$, and $\beta=\sqrt{5}/2$.

shows that this curve cannot be considered a shortcut (it is probably falling into the naked singularity).

V. CONCLUSIONS

We have considered here again the question of shortcuts in a Universe described by a membrane embedded in a bulk with two extra dimensions, the so-called dowain wall, described by Einstein gravity with a scalar field. In Ref. [18] the full set of solutions of the brane equation of motion and Israel conditions at the wall has been obtained. We studied the possibility of shortcuts in those cases. In one of our previous works we found [3] that in a static brane embedded in a pure AdS space with a black hole (AdS-Schwarzschild, AdS-RN) shortcuts may appear if a certain range of parameters is chosen [11]. Later, we proved that in a dynamical brane universe shortcuts are actually quite common and may provide an alternative explanation to the horizon problem.

TABLE I. Domain-wall time τ and time delays $\Delta\tau$ for shortcuts appearing in type-II and type-III solutions.

Conditions	t	τ	$\Delta\tau$
Type-II shortcuts			
Fig. 6, $v(0)=-3050$	7.5×10^{-5}	0.0025	0.0466
Fig. 6, $v(0)=-1000$	4.4×10^{-5}	0.0014	0.0027
Type-III shortcuts			
Fig. 10, $v(0)=0.145$	1.49	0.970	0.210
Fig. 10, $v(0)=0.140$	1.75	1.394	0.523
Fig. 11, $v(0)=-5\times10^4$	0.58	353	3.51
Fig. 11, $v(0)=-10^5$	1.11	683	26.6
Fig. 11, $v(0)=-1.2\times10^5$	1.33	823	48.1
Fig. 11, $v(0)=-1.5\times10^5$	1.69	1058	104
Fig. 13, $v(0)=-0.8$	0.73	0.753	0.123
Fig. 13, $v(0)=-0.9$	0.78	0.808	0.148
Fig. 13, $v(0)=-1$	0.81	0.842	0.111
Fig. 13, $v(0)=-1.04$	0.80	0.831	−0.129
Fig. 14, $v(0)=-5\times10^4$	0.61	372	4.11
Fig. 14, $v(0)=-10^5$	1.14	703	29.2
Fig. 14, $v(0)=-1.5\times10^5$	1.72	1081	112
Fig. 14, $v(0)=-2\times10^5$	2.42	1568	354

Indeed, if gravitational shortcuts are common before nucleosynthesis in a realistic model, they may provide an alternative to inflation in order to thermalize the early universe. In the present model, where the Universe is replaced by a domain wall, we have proved that shortcuts may exist and above all are abundant, which is a necessary condition in order to solve the homogeneity problem.

This is not sufficient though and further considerations in a more realistic setup are certainly needed. We should also stress that a time-varying dilaton could generate a detectable variation of the Newton constant, which imposes certain constraints on the parameters of the present model.

However, in spite of its shortcomings, the model shows interesting results. Moreover, we further show that the delay of the time of flight inside the brane may be comparable with the time of flight of the graviton itself. This lends further support for a thermalization via graviton exchange through extra dimensions, though still not a proof of the solution of the problem.

The question to be answered now is whether more realistic models including, e.g., further extra dimensions, such as in the Horava-Witten formulation, can display similar features.

ACKNOWLEDGMENTS

This work has been supported by Fundação de Amparo à Pesquisa do Estado de São Paulo (FAPESP) and Conselho Nacional de Desenvolvimento Científico e Tecnológico (CNPq), Brazil.

[1] M. Gasperini and G. Veneziano, Phys. Rep. **373**, 1 (2003).
[2] J. Polchinski, *Superstring Theory* (Cambridge University Press, Cambridge, England, 1998), Vols. 1 and 2.
[3] E. Abdalla, A. Casali, and B. Cuadros-Melgar, Nucl. Phys. **B644**, 201 (2002).
[4] C. Csáki, J. Erlich, and C. Grojean, Nucl. Phys. **B604**, 312 (2001).
[5] H. Ishihara, Phys. Rev. Lett. **86**, 381 (2001).
[6] R. Caldwell and D. Langlois, Phys. Lett. B **511**, 129 (2001).
[7] D. J. Chung and K. Freese, Phys. Rev. D **62**, 063513 (2000); **61**, 023511 (2000).
[8] E. Abdalla, B. Cuadros-Melgar, S. Feng, and B. Wang, Phys. Rev. D **65**, 083512 (2002).
[9] G. Starkman, D. Stojkovic, and M. Trodden, Phys. Rev. Lett. **87**, 231303 (2001); Phys. Rev. D **63**, 103511 (2001).
[10] D. J. Chung and K. Freese, Phys. Rev. D (to be published), astro-ph/0202066.
[11] E. Abdalla and A. G. Casali, hep-th/0208008.
[12] J. W. Moffat, hep-th/0208122.
[13] E. W. Kolb and M. S. Turner, *The Early Universe* (Addison-Wesley, Reading, MA, 1990).
[14] G. Giudice, E. Kolb, J. Lesgourgues, and A. Riotto, Phys. Rev. D **66**, 083512 (2002).
[15] Shin'ichi Nojiri, Sergei D. Odintsov, and Akio Sugamoto, Mod. Phys. Lett. A **17**, 1269 (2002); Shin'ichi Nojiri and Sergei D. Odintsov, J. High Energy Phys. **12**, 033 (2001); Bin Wang, Elcio Abdalla, and Ru-Keng Su, Mod. Phys. Lett. A **17**, 23 (2002).
[16] G. Gibbons and S. Hawking, Phys. Rev. D **15**, 2738 (1977).
[17] W. Israel, Nuovo Cimento B **44**, 1 (1966); **48**, 463(E) (1967).
[18] H. A. Chamblin and H. S. Reall, Nucl. Phys. **B562**, 133 (1999).
[19] P. Binétruy, C. Deffayet, and D. Langlois, Nucl. Phys. **B565**, 269 (2000).
[20] C. Csáki, M. Graesser, C. Kolda, and J. Terning, Phys. Lett. B **462**, 34 (1999).
[21] J. Cline, C. Grosjean, and G. Servant, Phys. Rev. Lett. **83**, 4245 (1999).
[22] P. Binétruy, C. Deffayet, U. Ellwanger, and D. Langlois, Phys. Lett. B **477**, 285 (2000).
[23] P. de Bernardis *et al.*, Nature (London) **404**, 955 (2000); Astrophys. J. Lett. **536**, L63 (2000); R. Stompor *et al.*, *ibid.* **561**, L7 (2001).